DESIGN OF COMPACT METAL-MOUNTABLE
UHF RFID TAG ANTENNA

TAN JIUN IAN

**A project report submitted in partial fulfilment of the
requirements for the award of Bachelor of Engineering
(Honours) Electronic and Communication Engineering**

**Lee Kong Chian Faculty of Engineering and Science
Universiti Tunku Abdul Rahman**

April 2021

DECLARATION

I hereby declare that this project report is based on my original work except for citations and quotations which have been duly acknowledged. I also declare that it has not been previously and concurrently submitted for any other degree or award at UTAR or other institutions.

Signature :

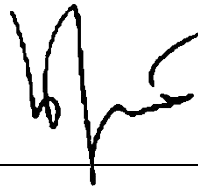Name : TAN JIUN IAN

ID No. : 17UEB01528

Date : 6-5-2021

APPROVAL FOR SUBMISSION

I certify that this project report entitled **"DESIGN OF COMPACT METAL-MOUNTABLE UHF RFID TAG ANTENNA"** was prepared by **TAN JIUN IAN** has met the required standard for submission in partial fulfilment of the requirements for the award of Bachelor of Engineering (Honours) Electronic and Communication Engineering at Universiti Tunku Abdul Rahman.

Approved by,

Signature   :

Supervisor   :   PROF TS DR. LIM ENG HOCK

Date   :   6-5-2021

Signature   :

Co-Supervisor :   DR. LEE YONG HONG

Date   :   6-5-2021

ACKNOWLEDGEMENTS

I would like to thank everyone who had contributed to the successful completion of this project. First of all, I would like to express my utmost thanks to my research supervisor, Prof Ts Dr. Lim Eng Hock as well as my co-supervisor Dr. Lee Yong Hong for assisting and guiding me throughout the development of the research. Their invaluable advice and enormous patience have contributed to the completion of this project.

Besides, I would also like to express my gratitude to my seniors. specifically Muthukannan Murugesh. They were willing to lead me a hand whenever I encountered problems in the final year project.

Also, I would like to hand in millions of thanks to my loving parents and friends who have given me encouragement and motivation throughout my final year project.

ABSTRACT

A new type of UHF RFID tag antenna, which consists of four elementary shorted patches, a feeding loop, and a ground plane, is proposed for designing a compact metal-mountable UHF RFID tag antenna. The feeding loop in Layer 2 is incorporated for exciting the shorted patches in Layer 1 and Layer 3 simultaneously through inductive coupling. The patches in Layer 1 and Layer 3 are tactfully combined with the narrow stubs before shorted to the ground plane through a shorting via. The narrow stubs are to provide additional inductance for this antenna to conjugate match with the chip impedance. As a result, a high power transmission coefficient of 93.5% is achieved. Apart from improving the matching level, the stubs are also very useful for tuning the resonant frequency to the desired UHF band. The tag antenna has a miniature size of 30 mm × 30 mm × 3.18 mm ($0.0914\ \lambda \times 0.0914\ \lambda \times 0.0096\ \lambda$). Despite being electrically small and low in profile, the proposed antenna can produce a stable omnidirectional radiation pattern when being mounted to a metal plate of 200 mm × 200 mm × 10 mm during the measurement process with the detection range up to 6.25 m. The tag has a stable resonant frequency of 914 MHz and it is not affected much by changes in the backing metal.

TABLE OF CONTENTS

LIST OF TABLES

LIST OF FIGURES

CHAPTER 1

INTRODUCTION

1.1 General Introduction

For the past two decades, Radio-Frequency Identification (RFID) technology has been an increasing need in the field of wireless communication due to the advantages such as higher reading distance, better safety performance, faster-reading speed, and greater capacity (Zhang, et al., 2019). With reference to Figure 1.1, a typical RFID system has a reader to collect and process the information of the tagged object, which is electronically stored in the tag. In recent years, there is a rapid growth of applying RFID antennas in the ultrahigh-frequency range (UHF) which is 860−960 MHz (Saba, et al., 2012). The tagging system of UHF RFID has gained prestige in many commercial applications such as remote access and inventory tracking due to it can provide a larger reading distance and higher memory capacity than others (Lee, et al., 2019; Ng, et al., 2019). It is also able to overcome those disadvantages faced by traditional bar-code systems. Hence, UHF RFID is playing a significant role in the RFID area.
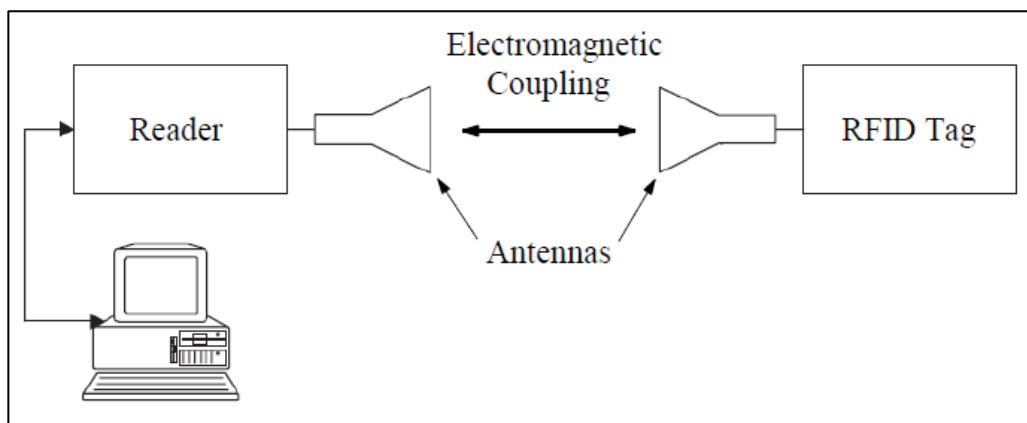
Figure 1.1: Radio-frequency communication in a typical RFID system.

Most of the application of UHF RFID is desirable to have the tag antenna that functions effectively when being mounted onto different surfaces such as plastic, wood, and metal surface (Althobaiti, et al., 2020; Erman, et al., 2020). However, those challenging surfaces can affect the tag's performance. Usually, a UHF RFID that is mounted onto a metal surface will cause the image current to deteriorate the radiation performance of the antenna. Besides, the coupling between the UHF RFID and the backing metal can deteriorate the performance of the tag as well (Lee, et al., 2020).

Usually, a UHF RFID tag antenna with an omnidirectional radiation pattern is preferable in the industry application. This is mainly due to omnidirectional tag antennas that can provide full spatial coverage in the azimuth plane (Lee, et al., 2020). In recent years, an omnidirectional antenna can be easily found in the wireless communication system. They play a major role and have high demand in many other systems, such as base stations and wireless local area networks (He, et al., 2020). Also, this type of tag antenna can provide higher reading speed and greater memory capacity, resulting in high demand in industrial applications such as retail management and supply chain management (Lee, et al., 2019).

1.2 Importance of the Study

The results of this present study may have a significant impact on providing a better radiation performance of the UHF RFID tag antenna in metal-mountable applications. Recently, the firth-generation of mobile communication networks (5G) has been appearing in sensing and identification applications (Althobaiti, et al., 2020). This shows autonomous and contactless environments have gained prestige in many industrial applications. A UHF RFID tag antenna with an omnidirectional radiation pattern for metal-mountable applications will become a breakthrough and an important milestone in the development of RFID technology and wireless communication system.

1.3   Problem Statement

In the past few years, different types of antenna structures have been developed and proposed to optimize the performance of metal-mountable applications. Planar-type UHF RFID is one of the useful techniques for designing tag antennas in this application. However, when a planar-type tag antenna is tagged on a metal surface, the radiation pattern will usually lose its original omnidirectional characteristic and result in a directional pattern. Recently, there are only a few existing on-metal UHF RFID tag antennas are capable to produce omnidirectional radiation pattern when attached to metallic surfaces, but they are still having a large dimension. Most of the on-metal tag antennas are not able to provide full coverage as they can only produce a directional radiation pattern when being mounted on the metallic object.

1.4   Aim and Objectives

The overall objective of this study is to propose a new low-profile UHF RFID tag antenna that is metal-mountable. The radiation pattern of this antenna is omnidirectional as it can provide full spatial coverage. This antenna has a miniature size and low profile, which is suited well for most industrial tagging applications.

The research aim is to design a compact on-metal tag antenna that can provide full spatial sensing in the azimuth plane. The objectives of the project are:
- To research and develop a compact tag antenna that can have read distance beyond 5 meter in all directions in the azimuth plane when mounted on metallic surfaces.
- To analyse and tune the input impedance of the tag antenna for achieving a conjugate match with the chip impedance.

1.5   Contribution of the Study

Metal-mountable tag antennas are usually directive antennas due to the reflective nature of the conducting platform underneath. As such, a miniature tag antenna that has an omnidirectional radiation pattern when mounted on metal will surely broaden up the RFID tagging applications. Thus far, there are only a few existing omnidirectional tag antennas that are electrically small and yet capable to achieve good omnidirectional performance on metallic objects.

In this study, the proposed compact tag antenna is also electrically small with a size of 30.00 mm $\times$ 30.00 mm $\times$ 3.18 mm (0.0914 λ $\times$ 0.0914 λ $\times$ 0.0096 λ), and able to provide full spatial coverage up to 6.25 m when it is tagged on metallic objects. The proposed antenna is having a smaller size compared with this type of existing antennas. Therefore, this study will further increase the market demand in the autonomous and contactless environment, such as a smart warehouse as shown in Figure 1.2. By using this project to achieve the smart city concept, there will always be digital interaction between people such as broadcasting and receiving important information to and from the masses.
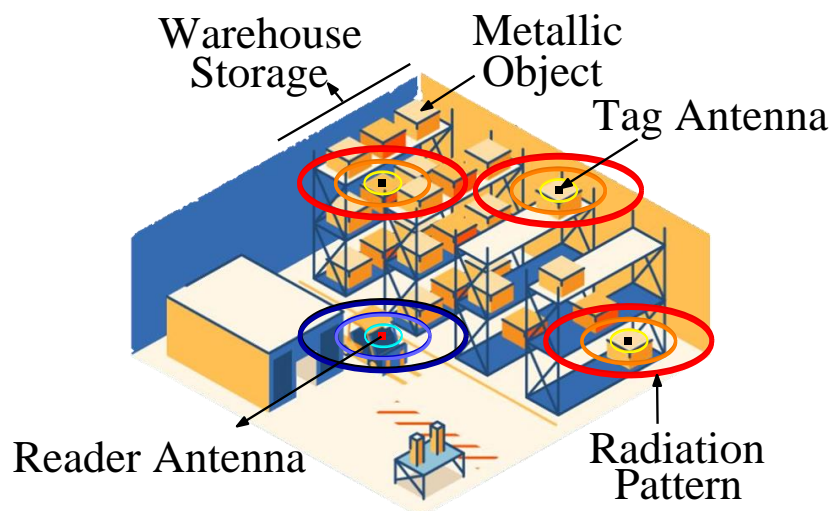
Figure 1.2: Smart warehouse management system utilising the omnidirectional characteristics of the proposed tag antenna.

1.6   Outline of the Report

This report is prepared in the following way. In Chapter 2, the literature review is discussed and existing solutions are discussed. The project planning and antenna configuration are described in Chapter 3. The simulated results of the tag antenna are studied in Chapter 4, along with parametric analysis for analyzing the antenna impedance. At last, the conclusion and recommendations for future work are discussed in Chapter 5.

CHAPTER 2

LITERATURE REVIEW

2.1 Introduction

The objective and aim of this study are to propose a new technical structure of an omnidirectional UHF RFID compact tag antenna that is suitable for the metal-mountable application. Therefore, relevant background knowledge of this study needed to be reviewed, so that can a perfectly working UHF RFID tag antenna can be designed.

2.2 RFID Tag Antennas Review

Radio-Frequency Identification (RFID) is one of the Auto Identification (Auto-ID) technologies, which utilizes electromagnetic fields and waves to track and identify objects automatically. Since the firth-generation of mobile communication networks (5G) has been introduced into the world recently, the ultrahigh-frequency range (UHF) RFID has gained prestige in many commercial applications such as retail management (Lee, et al., 2020), logistics tracking (Lee, et al., 2019), transportation (Bong, et al., 2017), and remote access (Ng, et al., 2019). Most of the applications require the UHF RFID tag antenna to be small size, low profile, and also functioning stably when being mounted onto different surfaces such as safety glasses (Lin, et al., 2012), water bottles (Bjorninen, et al., 2011), and particularly on the metal surface. This is because on-metal application will cause the image current to deteriorate the antenna's efficiency (Lee, et al., 2019) and degenerate the antenna's performance. The antenna performance is heavily affected by some important parameters, such as antenna gain, read distance, radiation efficiency, resonant frequency, S-parameter, and bandwidth of the antenna.

2.3   Directional and Omnidirectional Antennas

Antennas can be categorized into directional and omnidirectional antennas. This classification relies on the beamwidth directionality of antennas. Beamwidth is the angular separation between 3dB points of the antenna radiation pattern, also known as the antenna radiation coverage area which is measured in degrees (Cisco, 2007). Figure 2.1 illustrated the communication ranges of directional transmission and omnidirectional transmission.
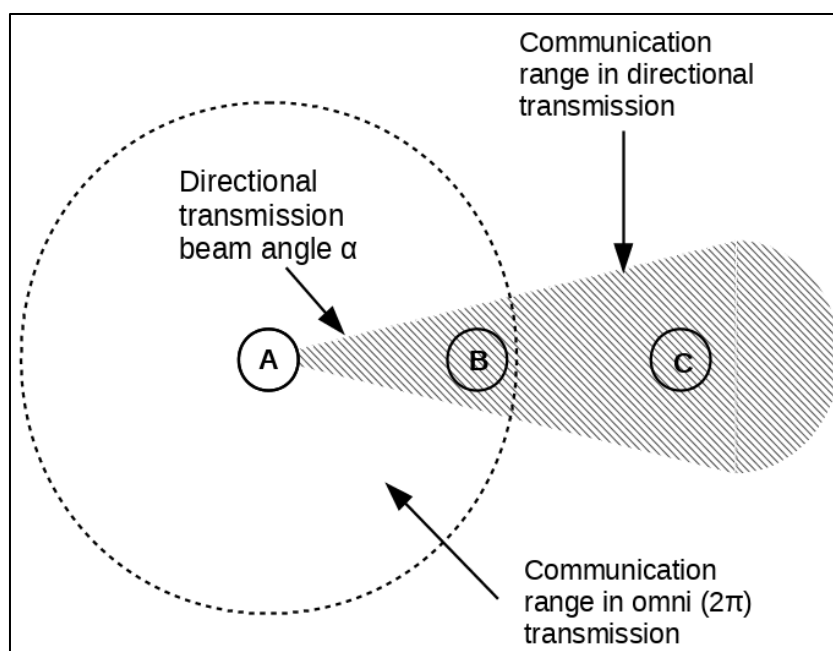
Figure 2.1: Communication ranges for directional and omnidirectional antennas.

A directional antenna is an antenna that can cover with long reading distance, but with less effective beamwidth. The basic function of it will be diverting the radio-frequency energy in a particular direction (Cisco, 2007). However, this type of antenna is only suitable in low line-of-sight (LOS) coverage, it is widely used in isle structures with spaces in between. The disadvantage of a directional antenna is not able to have a large area coverage due to its angular coverage is less. When the gain of a directional antenna increases, the radiation angle will reduce, resulting in a long coverage distance but with a low coverage angle.

An omnidirectional antenna is an antenna that can radiate power in all directions in the azimuth plane. The basic function of it will be pushing in the energy lobes from the top and bottom, resulting in a doughnut type pattern (Cisco, 2007). Since this type of antennas covers up 360 degrees of horizontal pattern, it is very convenient to attach to the product. When the gain of an omnidirectional antenna increases, it will result in a larger horizontal coverage and narrower vertical beamwidth. However, there will be no coverage below the antenna. In this case, the omnidirectional antenna is suitable for a broad coverage communication system.

Since antennas are becoming ubiquitous in various fields, there are different types of tag antennas that have been designed for on-metal applications. However, most of the designed on-metal tag antennas can only produce a directional radiation pattern. Usually, a tag antenna with an omnidirectional radiation pattern is more preferable to the directional antenna in industry applications. This is because an omnidirectional tag antenna can be widely used in industrial applications that require sensing detection covers up to 360 degrees in the azimuth plane. Therefore, the proposed compact tag antenna structure that having omnidirectional characteristics and applicable for metal-mountable applications will become a breakthrough and an important milestone in the development of RFID technology.

2.4   Antenna Gain and Read Distance

The antenna gain is referred to as the ratio of the radiated far-field power produced by the particular antenna with the radiated power produced by an isotropic antenna. The isotropic antenna radiates power equally in all directions. It is the hypothetical lossless antenna that is not practical in industrial applications. The read distance of the antenna is also closely related to the antenna gain. The higher the antenna gain, the longer the read distance of the antenna. However, if the size of the antenna is electrically small, then the antenna gain will have a fundamental limit, the given formula is illustrated in (Andrew, et al., 2008).

2.5   Radiation Efficiency

The radiation efficiency of the antenna represents how well the antenna can convert the input power to radiated power. It is a measurement of electromagnetic energy to determine antenna performance. However, the radiation efficiency will also have a fundamental limit for an electrically small antenna according to (Morteza, et al., 2018).

2.6   Resonant Frequency

Refer to (ECS, 2021), a resonant frequency of an antenna is the frequency when the antenna can store and transfer energy between different storage modes effectively. With the reference to Figure 2.2 (Electronic notes, 2021), the resonant frequency is the frequency when an antenna shows purely resistive. At this point, the capacitance and inductance of the antenna cancel each other out, resulting in a combination of radiation resistance and loss resistance. Also, the antenna size will affect the resonant frequency. The bigger the antenna size, the lower the resonant frequency. In this project, the proposed antenna is designed to have a good radiation pattern with good realized gain at the UHF band which is 860−960 MHz. Therefore, the resonant frequency of the designed antenna should be allocated at the range within 860 MHz and 960 MHz.
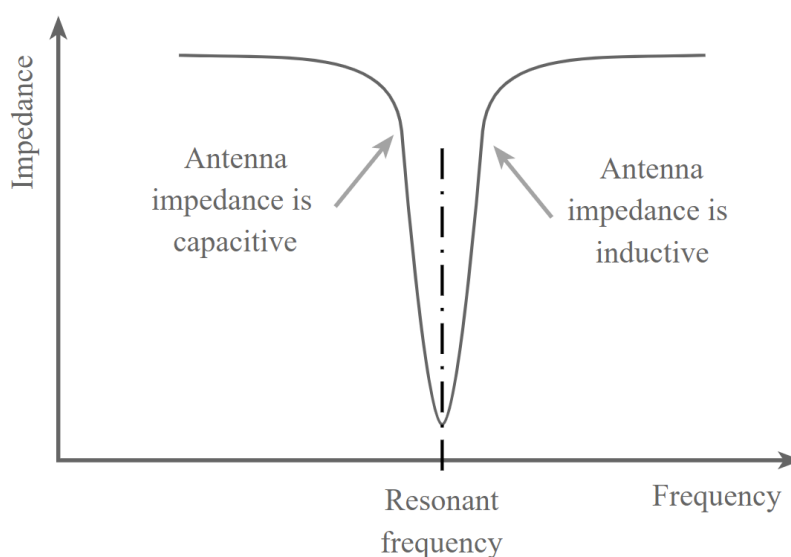
Figure 2.2: Resonant frequency of an antenna. (Electronic notes, 2021)

2.7 S-Parameter and Bandwidth

A scattering parameter (S-parameter) is a technique to describe the relationships of input ports and output ports of the antenna. For a two ports system, the S-parameters that will be considered are S_{11}, S_{12}, S_{21}, and S_{22}. S_{12} and S_{21} are both defined as the voltage gain, where S_{12} is reverse voltage gain and S_{21} is forward voltage gain. On the other hand, S_{11} and S_{22} are referred to as the reflection coefficient, where S_{11} is the input port and S_{22} is the output port. S_{11} will show a negative decibel value when there are some power is being transmitted from the antenna. However, if all the radiated power of the antenna is fully reflected, the S_{11} is said to be 0 decibels. Figure 2.3 illustrates an example of S_{11} against the frequency (Carla, et al., 2009).
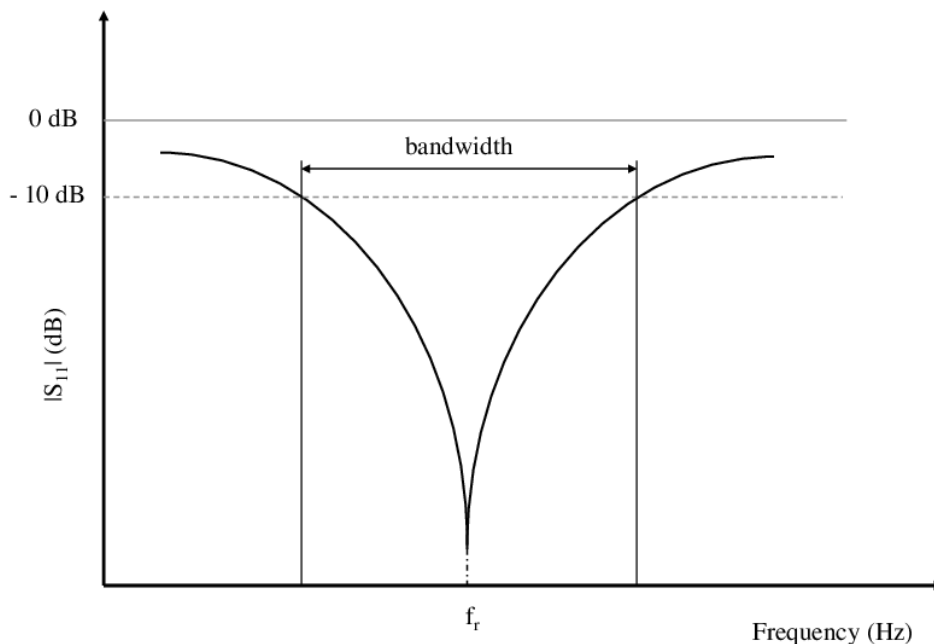
Figure 2.3: Graph of S_{11} against the frequency. (Carla, et al., 2009)

Refer to Figure 2.3 again, the antenna operation bandwidth can also be observed in the graph of S_{11} against the frequency. Antenna bandwidth represents the working frequency range of the antenna. It is said to be the antenna bandwidth for the frequencies range below -10 dB of S_{11}.

2.8   Existing Solutions

Despite the fact that there are some new antenna structures that have been introduced for on-metal applications in the past few years, most of them can only produce directional radiation patterns. In recent years, there are only a few UHF RFID tag antennas such as compact magnetic loop antenna (Lee, et al., 2020) and loop-fed planar inverted-L antenna (Lee, at al., 2020) are capable to produce omnidirectional radiation patterns when attached to metallic surfaces but they are still large in size. Usually, a typical omnidirectional antenna is not able to function well when being mounted onto a metal surface due to the effect of image current. In compact folded dipole with embedded matching loop antenna (Bong, et al., 2017) and meandered dipole antenna with the slotted ground (Zhang, et al., 2017), their tag antennas are able to produce an omnidirectional radiation pattern in free space. However, such antennas will become directional antennas with a reduced antenna gain and reading distance when attached to a metallic surface. Also, in the planar inverted-L antenna with dielectric resonator feed (Lin, et al., 2009), the concept of PILA is used to design an omnidirectional antenna for mobile handsets, but the antenna will also lose its omnidirectional characteristic when being mounted on a metallic surface.

One of the ways to improve on-metal antenna gain is using a star-shaped slot with an embedded terminal-grounded L-shaped feedline and attached it to a huge ground plane, as shown in the Compact RFID antenna with embedded feed network (Pan, et al., 2014). Also, in a Low-profile PIFA array antenna (Chen, et al., 2010), the reading distance can be improved by using multiple PIFAs to create an array antenna. These two types of RFID tag antennas are good ways to improve the performance of on-metal antenna tags, but they are still resulting in a directional radiation pattern.

2.8.1   Metal-Mountable Tag Antenna

Compact Folded C-shaped Antenna

In this paper, a compact antenna named compact folded C-shaped antenna is proposed for on-metal applications as illustrated in Figure 2.4. This antenna is a combination of the loop antenna and planar inverted-L antenna (PILA). The PILA structure in this article is incorporating with the loop antenna and resulting in improved radiation efficiency (Lee, et al., 2019).
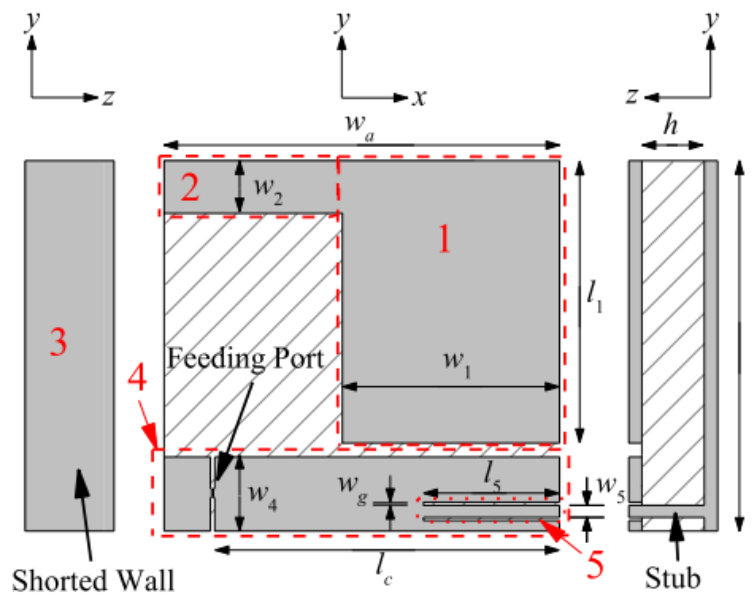
Figure 2.4: Compact folded C-shaped antenna. (Lee, et al., 2019)

This antenna produces a directional radiation pattern with a realized gain of −3.77dB at the resonant frequency of 915 MHz when being mounted on a metallic surface. The strength of this antenna is simple to design and easy to fabricate. By comparing to the ordinary loop antenna, the loop antenna structure on this paper is added with a horizontal portion of the inductive stub. (Lee, et al., 2019) The result shows a greater magnetic field intensity appears around this stub, hence it improves the inductance of the compact antenna. The size of the antenna is 40 mm × 40 mm × 1.6 mm. This on-metal tag antenna design has solved the problem of image current degeneration. However, it only can produce a directional radiation pattern, which cannot provide full spatial coverage.

The planar inverted-L antenna (PILA) structure mentioned in this article is one of the earliest low profile antennas. PILA is one of the common types of monopole antenna as shown in Figure 2.5. (Puri, et al., 2014). However, the PILA structure always suffers a higher mismatching loss due to it has high input reactance and low input resistance (Alja'afreh, et al., 2014). This problem makes PILA less attractive for low profile and small antenna design.
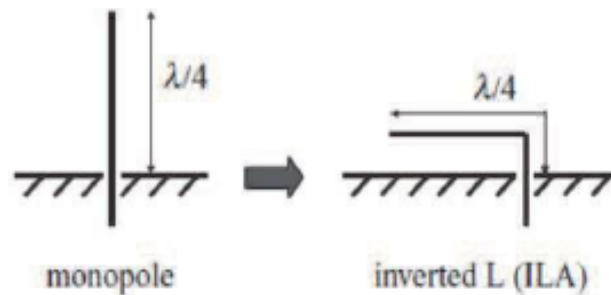
Figure 2.5: General concept of PILA. (Puri, et al., 2014)

Miniature PIFA Patch Antenna

To overcome the problem faced in the PILA structure, a different type of structure named planar inverted-F antenna (PIFA) is proposed. The PIFA is converted from PILA by increasing a short strip to improve the radiation characteristics (Dakhli, et al., 2019). A PIFA is grounded at the base and fed at some intermediate point as shown in Figure 2.6 (Puri, et al., 2014). The PIFA can achieve better matching without a matching network.

Figure 2.6: General concept of PIFA. (Puri, et al., 2014)

In this article, the planar inverted-F antenna (PIFA) is presented to achieve miniaturization (Lee, et al., 2018). The antenna structure of this paper is using two F-shaped patches by placing them side-by-side, and the patch on the left is the inversion of that on the right side as shown in Figure 2.7. The tag antenna structure is 32 mm × 35 mm ×1.6 mm.
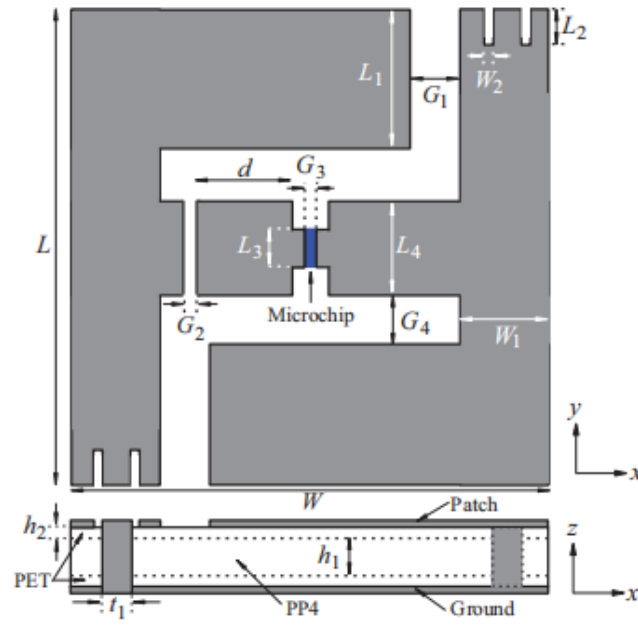
Figure 2.7: Miniature PIFA patch antenna. (Lee, et al., 2018)

The antenna structure is simple and having a good impedance matching without adding any extra matching network while it is mounted on a metal plate of 200 mm × 200 mm × 10 mm. Compared to other conventional types of antenna, this antenna does not require multiple shorting vias and stacked patches. This antenna can achieve a reading distance of 8.7 m with a directional radiation pattern when being mounted on a metallic surface at the resonant frequency of 904 MHz. Similar to most of the on-metal tag antennas, they are not able to provide full spatial coverage.

2.8.2 Omnidirectional Tag Antenna

Meandered Dipole Antenna with Slotted Ground

A modifiable quarter-wavelength meandered dipole is proposed to produce an omnidirectional radiation pattern free space as illustrated in Figures 2.8(a) and 2.8(b) (Zhang, et al., 2017). An adjustable T-matching network antenna and a slotted ground are used in the proposed tag antenna to achieve an omnidirectional radiation pattern with good antenna gain. Omnidirectional antennas usually have lower gain compared with directional antennas. Directional antennas can divert all the radiated energy in a particular direction. However, omnidirectional antennas will push in the energy from top and bottom, resulting in a doughnut shape radiation pattern with a lower gain value. T-matching networks that are used in this paper can significantly improve the gain of the omnidirectional antenna.

(a)

(b)
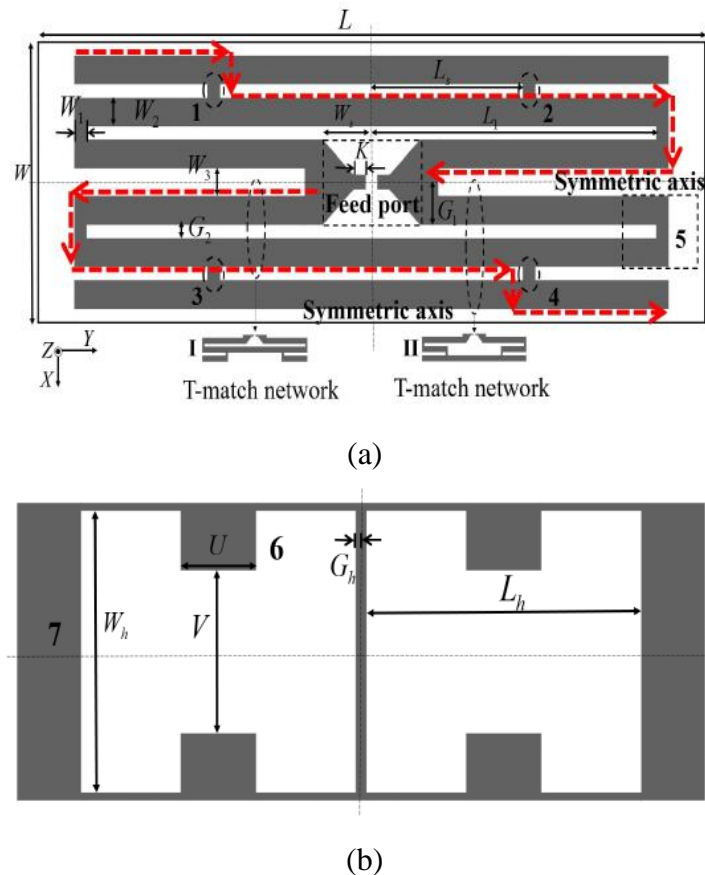
Figure 2.8: (a) Top view and (b) Bottom view of the antenna. (Zhang, et al., 2017)

This antenna is having a compact size and produces an omnidirectional radiation pattern in the free space as illustrated in Figure 2.9. However, when it is being mounted at a metallic surface, the radiation pattern becomes directional as shown in Figure 2.10. This shows that the omnidirectional antenna loses its characteristics, resulting in a directional radiation pattern with a reduced antenna gain. However, this antenna structure is still an appropriate reference for designing an on-metal omnidirectional tag antenna.
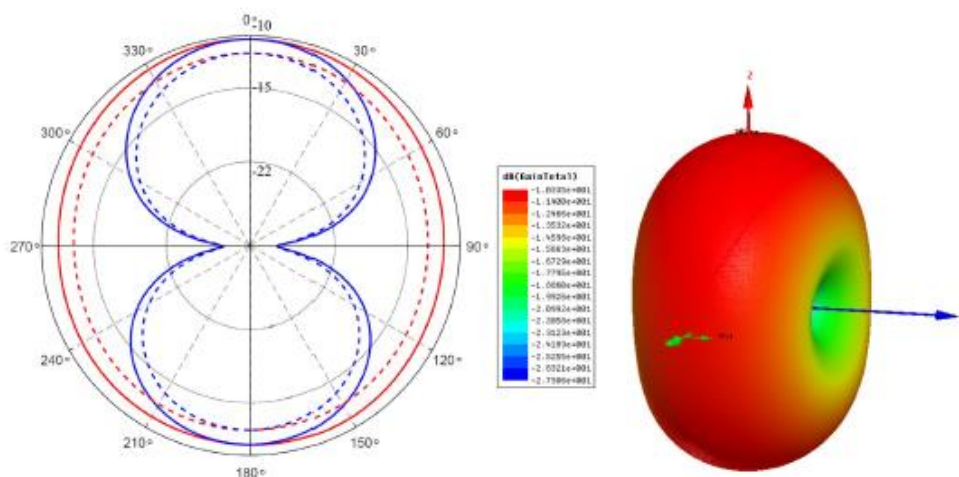
Figure 2.9: Radiation pattern in free space. (Zhang, et al., 2017)
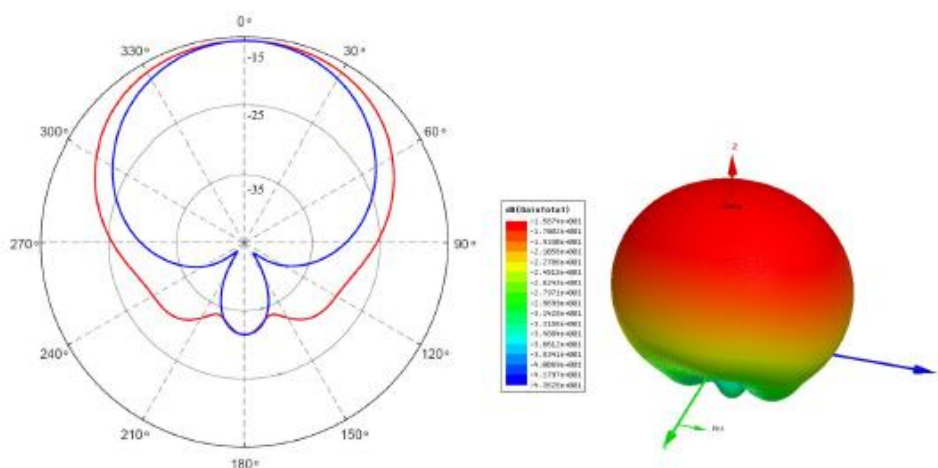
Figure 2.10: Radiation pattern when mounted on a metallic surface. (Zhang, et al., 2017)

PILA with Dielectric Resonator Feed

In this paper, a multiband PILA fed by a microstrip line is designed for mobile devices communication operation purposes such as GSM and DCS. The PILA produces a multiband result by making use of a ceramic resonant coupling feed to excite it. The coupling feed mechanism has consisted of an open-end microstrip feed line and a coupling dielectric resonant disk as shown in Figure 2.11 (Lin, et al., 2009).

The radiation pattern in the free space of this antenna is omnidirectional and has a gain of −9dBi at the resonant frequency of 925 MHz. Similar to the quarter-wavelength meandered dipole antenna (Zhang, et al., 2017) as mentioned above, if the antenna is positioned at a metallic surface, it will produce a directional radiation pattern with a reduced antenna gain.
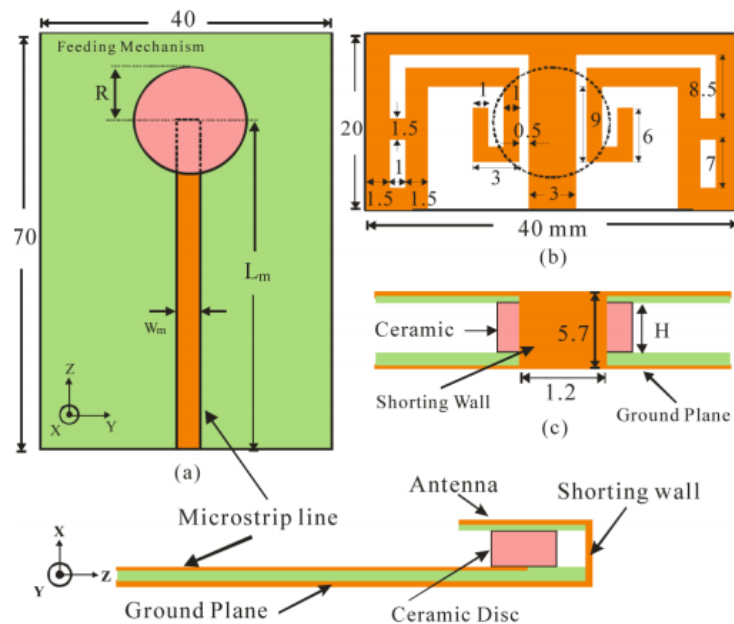
Figure 2.11: PILA with dielectric resonator feed. (Lin, et al., 2009)

2.8.3 On-Metal Omnidirectional Tag Antenna

Compact Magnetic Loop Antenna

In this paper, for the first time, an omnidirectional UHF RFID antenna is designed for on-metal applications. This technique is using the concept of a magnetic loop source together with an annular slot exciter to design a magnetic loop antenna. This compact antenna is able to function well and produces an omnidirectional radiation pattern in the far-field region with a small size of 38 mm × 38 mm × 1.6 mm (Lee, et al., 2020).

Figure 2.12 shows the structure of this antenna comprised of a shorted patch, annular slot exciter, shorting stubs, and notches (Lee, et al., 2020). The notches in the antenna structure are important as they can reduce the gain fluctuation and bring down the operating frequency to the desired range with is UHF band. The antenna is having a high transmission coefficient and a long reading distance of more than 5 meters. The concept of using notches to bring down resonant frequency is used as a reference when designing the proposed antenna.
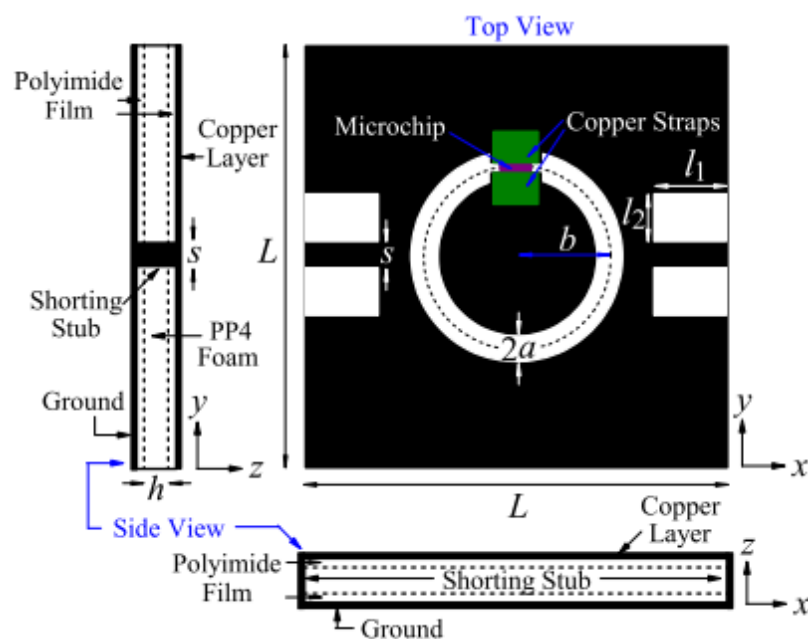
Figure 2.12: Compact magnetic loop antenna. (Lee, et al., 2020)

Loop Fed Planar Inverted-L Antenna

In this article, there are four identical planer inverted-L antennas (PILA) placing together to form a new type of UHF on-metal compact tag antenna (Lee, et al., 2020). The radiation pattern also shows omnidirectional which provides great coverage in the azimuth plane. The four PILAs are located in a rotational symmetry constellation and all are excited by a circular loop as illustrated in Figure 2.13.
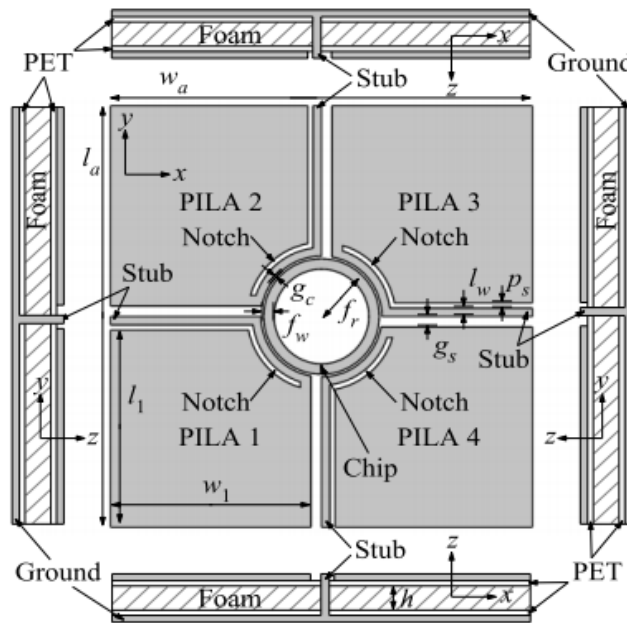
Figure 2.13: Loop fed planar inverted-L antenna. (Lee, et al., 2020)

The circular feeding loop introduced an extra reactance to the tag antenna for enhancing the impedance matching with the RFID microchip (Lee, et al., 2020). Compared with the Compact magnetic loop antenna which has mentioned above, this antenna has a slightly bigger size of 40 mm × 40 mm × 1.6 mm. However, the reading distance is also slightly longer than it which is 5.9 m. The omnidirectional gain has been achieved −6dBi in the UHF band. The electric field is strong around the patch edges, and the magnetic field is strong at the center. The circular feeding loop which introduced additional reactance in this antenna is also used as a reference later for devising the proposed antenna.

CHAPTER 3

METHODOLOGY AND WORK PLAN

3.1 Introduction

In this project, an electromagnetic waves simulator (CST Microwave Studio) is used for designing the proposed antenna. CST simulation will be done to develop and optimize the omnidirectional tag antenna. The impedance characteristics and radiation performance of the proposed antenna can be monitored in the software. In this chapter, project planning and antenna configuration will be discussed in detail.

3.2 Project Planning

This project can be categorized into three parts. In the first part, the omnidirectional UHF RFID tag is designed and optimized using CST Microwave Studio. In the second part, the parameters of the designed antenna are optimized using a conventional optimizer so that the tag can demonstrate a good omnidirectional radiation pattern when tagged on metal and in the metallic cavity. Lastly, the prototypes are fabricated and measured in the third part.

The ultimate objective of this study is to propose a new antenna UHF RFID tag antenna structure that produces an omnidirectional radiation pattern. To ensure the project can be completed on time, a Gantt chart of the working plan has to be scheduled at the beginning. The project tasks are displayed against the time in Table 3.1.

Table 3.1: Gantt chart.

	Tasks	Jun 2020	Jul 2020	Aug 2020	Sep 2020	Oct 2020	Nov 2020	Dec 2020	Jan 2021	Feb 2021	Mar 2021	Apr 2021
Part 1	Reviewing past works for UHF RFID tags that have omnidirectional radiation pattern.	▓										
	Designing omnidirectional tag antenna.		▓	▓								
	Simulating and optimizing the electromagnetic model using the CST Microwave Studio.			▓	▓							
Part 2	Establishing a theoretical model for studying the radiation characteristics of the tag antenna that is used in close proximity to metallic object.					▓	▓					
	Analyzing the impedance characteristic of the optimized tag antenna.						▓	▓				
	Fabricating the prototypes of the optimal design.							▓	▓			
Part 3	Measuring the performances of the prototypes.									▓	▓	
	Report writing.										▓	▓

3.3 Antenna Configuration

The proposed antenna consists of four layers: two conductive layers, a feeding loop layer, and a ground layer. Figures 3.1 and 3.2 illustrate the configuration of the proposed antenna. Referring to Figure 3.1, all layers have the same dimension of $l_a \times w_a$ which are 30 mm $\times$ 30 mm. The two conductive layers are composed of four identical radiating patches. With reference to Figure 3.2, two patches are placed at the upper left and bottom right corner of Layer 1, and two patches are placed at the upper right and bottom left corner of Layer 3. The two patches in each layer are diagonally aligned and having identical dimensions of $w_p \times w_p$. Also, the two patches within the same layer are connected by a narrow stub (arc segment) before shorted to the ground plane through a shorting vertical interconnect access (via) (d = 0.5 mm). The narrow stubs are to provide additional inductance for this antenna to conjugate match with the chip impedance. For Layer 1 to Layer 3, the inlay is made by removing a lossy aluminium lamination (m = 0.009 mm) which was first deposited on a top surface of a thin polyethylene terephthalate (PET, 0.05 mm) film.
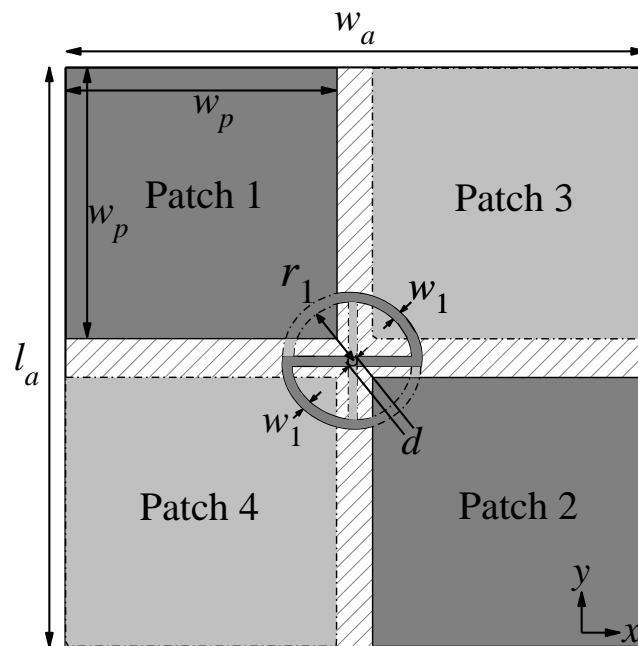

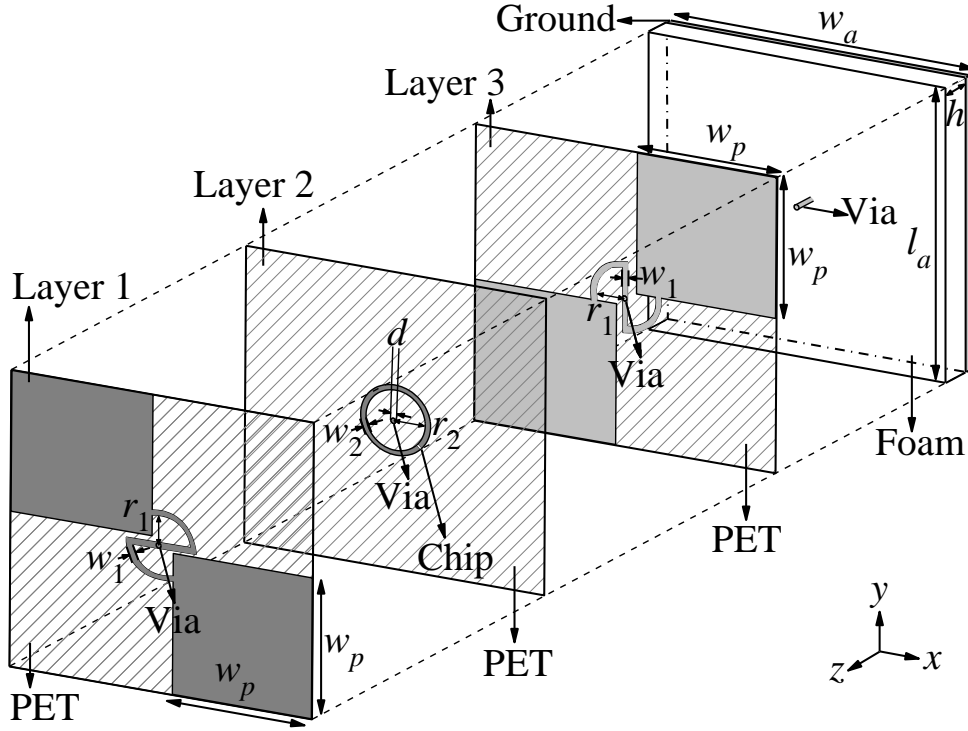Figure: 3.1: Top-down view of the proposed tag antenna configuration.

Figure 3.2: Assembly diagram of the proposed tag antenna configuration.

Referring to Figure 3.2 again, the metallic layer in Layer 2 is displayed as a concentric annular shape etched at the center of the PET. In this case, the annular shape aluminium acts as a circular feeding loop which functioning as a source to other layers of the antenna. Patches located in Layer 1 and Layer 3 are excited simultaneously by this circular feeding loop through inductive coupling. To achieve good impedance matching, the radius of the feeding loop is the same as the radius of arc segments located on Layer 1 and Layer 3. Also, a 0.15 mm narrow gap appears on the bottom right corner of the feeding loop is for accommodating the RFID microchip (UCODE 8) (UCODE, n.d.) which has a chip impedance of $13 - j191$ Ω at 915 MHz. The effects of changing the location angle of chip mounting are insignificant to the proposed tag antenna.

For the Ground layer, it comprises of a piece of square polyethylene foam ($\varepsilon_r = 1.06$, tan$\delta \sim 0.0001$) (ECCOSTOCK, n.d.) with a total substrate thickness of $h = 3.176$ mm. Also, an aluminum lamination with an electric conductivity of 3.72×10^7 S/m is placed underneath the bottom of the substrate functioning as a ground plane.

Finally, a Genetic Algorithm Optimizer of the CST Microwave Studio is used for optimizing the design parameters. Before the optimization process of the proposed antenna, some parameters are first fixed, such as $w_a = 30.00$ mm, $l_a = 30.00$ mm, $d = 0.5$ mm and $h = 3.176$ mm. Meanwhile, other parameters will obtain through the optimization process. The objective of the optimization is to obtain a good omnidirectional radiation pattern with a good realized gain at the desire UHF band. The optimization processes will be closed up when those objectives are met. During the simulation process, the designed tag antenna is located at the center of a piece of 200 mm $\times$ 200 mm $\times$ 10 mm copper plate since it is proposed to be used for metal-mountable applications. However, the effects of changing different sizes of the backing metal plate are less significant to the proposed tag antenna. The optimized parameters values are found after several simulations: $w_p = 14.00$ mm, $r_1 = 3.07$ mm, $r_2 = 3.07$ mm, $w_1 = 0.5$ mm, $w_2 = 0.5$ mm.

CHAPTER 4

RESULTS AND DISCUSSION

4.1   Introduction

In this chapter, the S-parameter, resonant frequency, input impedance, realized gain, currents distribution, and radiation pattern are studied and discussed. Also, parametric analysis for the proposed antenna is studied in this chapter for analyzing the impedance characteristics and radiation performance of the proposed antenna. The designed tag antenna is located at the center of a piece of 10×10 cm^2 copper plate during the simulation since it is proposed to be used for metal-mountable applications. A Genetic Algorithm Optimizer of the CST Microwave Studio is used to simulate the design parameters of the proposed antenna to achieve optimization.

4.2   Optimized Antenna Results

4.2.1   S-Parameter and Resonant Frequency

The S-parameter (S_{11}) of the proposed antenna is illustrated in Figure 4.1. It can be seen that the proposed tag antenna is having a reflection coefficient, S_{11} of -12.22 dB. This result shows good impedance matching is achieved between the chip and the proposed antenna. Refer to Figure 4.1 again, the resonant frequency of the tag antenna is 914 MHz. This is because the proposed tag antenna is purely resistive at the resonant frequency of 914 MHz, where the capacitance and inductance of the antenna cancel each other out. As a result, the proposed antenna can function well in the UHF band which is $860-960$ MHz.
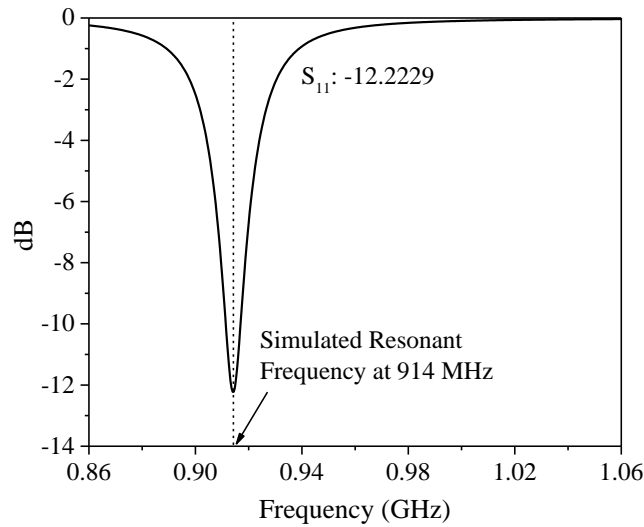
Figure 4.1: S-parameter and resonant frequency of the proposed antenna.

4.2.2 Input Impedance

The input impedance (Z-parameter) is also simulated by the CST software to obtain the changes of input impedance. Referring to Figure 4.2, the proposed antenna is having an input impedance of $7.9 + j191.3$ Ω at the resonant frequency of 914 MHz. The proposed antenna is using the microchip named UCODE 8, which has a chip impedance of $13 - j191$ Ω at 915 MHz. This result shows good impedance matching is attained and maximum power transfer has occurred between the chip and the proposed antenna.
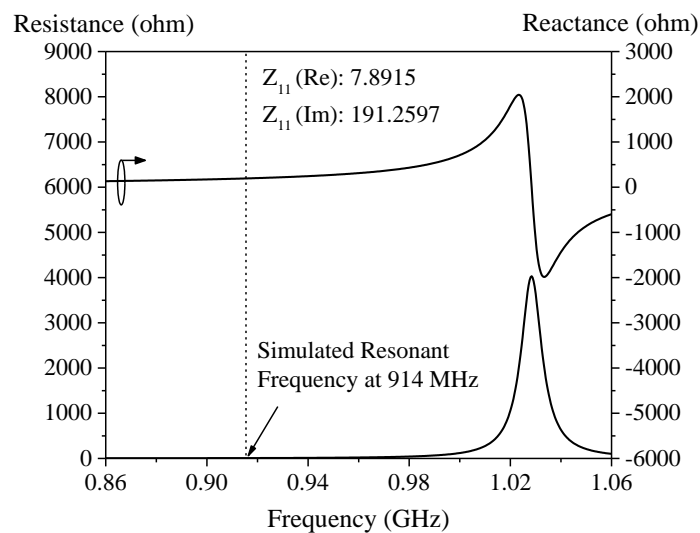

Figure 4.2: Input impedanceof the proposed antenna.

4.2.3 Power Transmission Coefficient

Good impedance matching can be further proven by referring to the power transmission coefficient of the proposed antenna as illustrated in Figure 4.3. The power transmission coefficient is 0.935 at the resonant frequency of 914 MHz. This shows the power transmission efficiency of the proposed antenna is 93.5% at 914 MHz. High power transmission efficiency is achieved because the proposed antenna has adequate resistance and inductive reactance to have good conjugate matching with the chip.
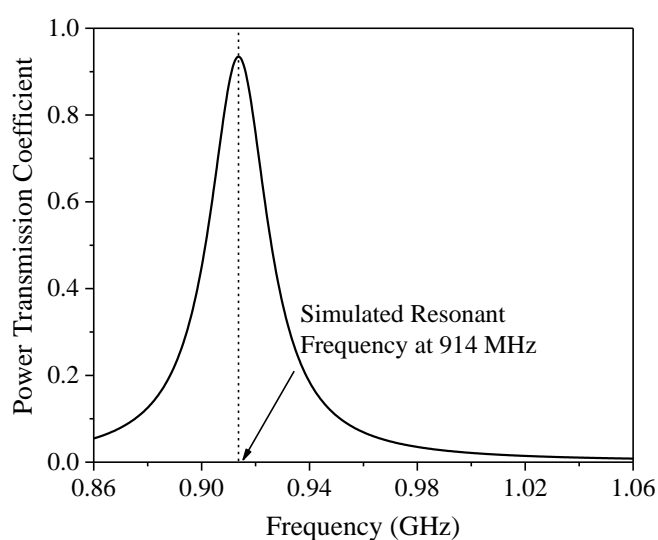

Figure 4.3: Power transmission coefficient of the proposed antenna.

4.2.4 Radiation Pattern and Read Distance

With reference to the radiation pattern in Figure 4.4, the tag antenna displayed a good omnidirectional characteristic in all directions in the azimuth plane. There is a constant antenna gain of -9.02 dBi at the resonant frequency of 914 MHz when it is tagged on a copper plate surface. In addition, it is also found that the radiation efficiency of the tag antenna, e_{cd} is 0.0847 at the resonant frequency of 914 MHz. It is an acceptable value for an electrically small antenna which only 30 mm $\times$ 30 mm $\times$ 3.18 mm. (Pfeiffer, et al., 2017) Also, When being mounted on a metal, the tag antenna is able to have an achievable read distance up to 6.25 m in all directions as shown in Figure 4.5.
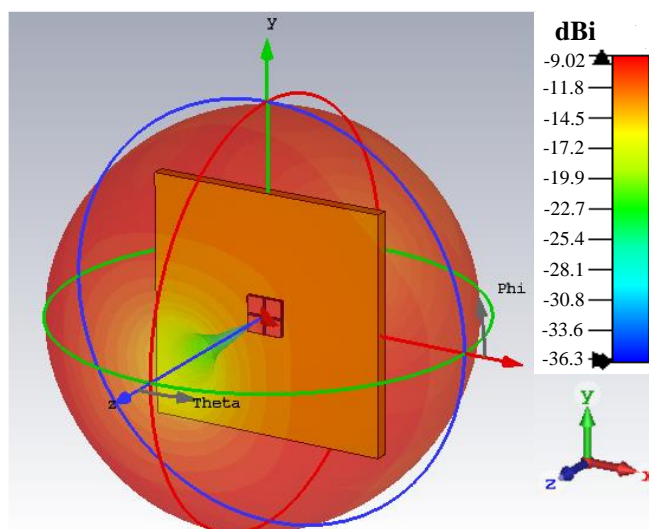
Figure 4.4: Simulated radiation pattern produced by the proposed antenna.
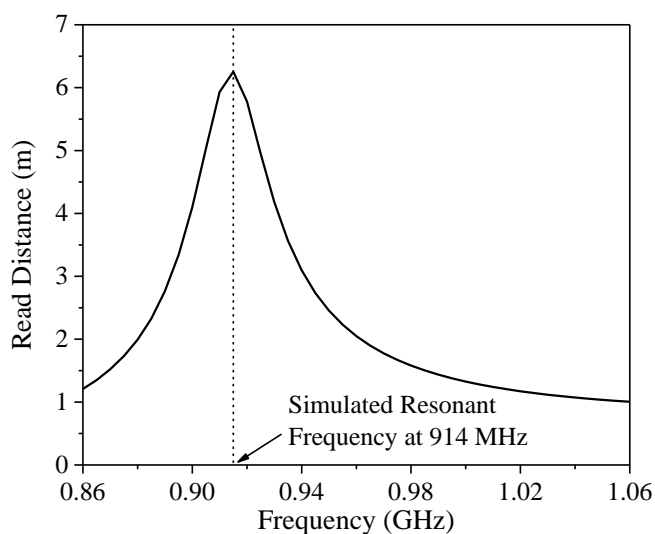
Figure 4.5: Achievable read distance of the proposed antenna.

4.2.5   Surface Currents Distribution

Figure 4.6(a) shows the top view surface currents distribution of the proposed tag antenna at the frequency of 914 MHz. With reference to Figure 4.6(b), high current densities are observed on both patches in Layer 1. Currents are flowing in and out between the patches and the arc segment, where the arc segment connects both patches together. Similar effects are also can be found in Layer 3 as illustrated in Figure 4.6(d). This is because Layer 1 and Layer 3 are having a similar structure and both layers are excited by the same feeding loop in Layer 2 simultaneously.

Figure 4.6(c) shows the currents distribution of the feeding loop in Layer 2. Currents concentrate on the upper left and bottom right corner at the top surface of the feeding loop. Also, for the bottom surface of the feeding loop, currents concentrate on the upper right and bottom left corner. This is because the feeding loop is located in the middle of both radiating layers, resulting in high current densities that can be found below each radiating patch.
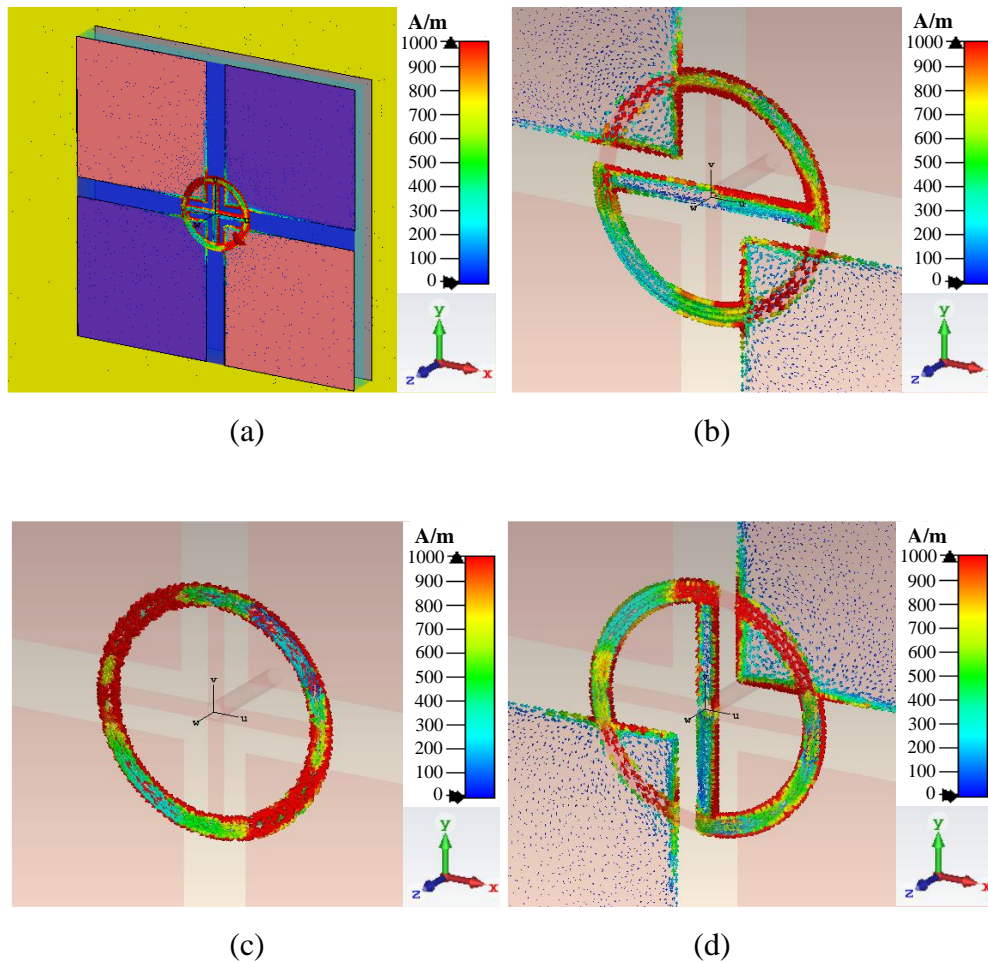

(a)

(b)

(c)

(d)

Figure 4.6: Surface currents distribution when tag antenna is placed on a 10×10 cm^2 copper plate at the resonant frequency of 914 MHz (a) top view, (b) Layer 1, (c) Layer 2, (d) Layer 3.

4.2.6   Electric and Magnetic Field Distribution

Also, it can be observed that the circular feeding loop in Layer 2 has effectively excited all four patches in Layer 1 and Layer 3, resulting in all four patches resonate in the same phase. To prove this, electric and magnetic field distributions are studied and simulated as shown in Figures 4.7(a) and 4.7(b) respectively.
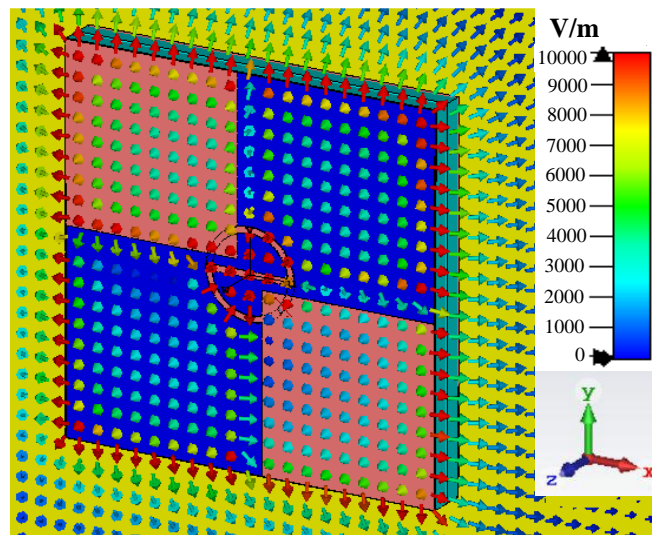
(a)
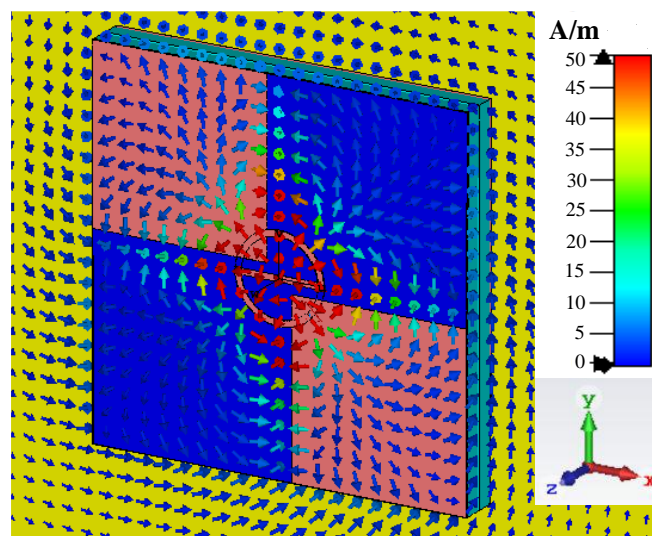
(b)

Figure 4.7: (a) Electric field and (b) magnetic field distributions of proposed tag antenna at the resonant frequency of 914 MHz.

Figure 4.7(a) shows the electric fields are found to be greater at the arc segments and all over the edges of the tag antenna. This is because the arc segments and edges are electrically opened which is reasonable to have strong electric fields. Besides, the pointing direction of the electric fields is normal to the patches. This contributes to the electrically small antenna less become influenced by the copper plate behind the tag antenna.

Stronger magnetic field intensities are observed at the center and the via of the tag antenna as illustrated in Figure 4.7(b). This shows that there is a good inductive coupling between all the arc segments (Layer 1 and Layer 3) and the circular feeding loop in Layer 2. Also, the via acts as an inductive shorting stub that connects each layer to the ground plane, resulting in strong magnetic fields occurred on it.

4.3 Parametric Analysis

4.3.1 Arc Segment Radius and Width

Subsequently, the parametric analysis is carried out to study the effects of the important design parameters. The effects of changing the radius of the arc segment in Layer 1 and Layer 3 are first studied and the changes of input impedance are shown in Figure 4.8. As shown in Figure 4.8, increasing the radius of arc segment (r_1) in both layers, introduces a tuning sensitivity of $\partial f/\partial r_1$ = −0.177 GHz/mm. The negative sign shows that the graph shifted left when the radius is increased. Also, this is useful for coarse-tuning purposes.

Similar effects are also observed in Figure 4.9 when the width of the arc segment (w_1) in Layer 1 and Layer 3 is increased while other parameters remain unchanged. The tuning sensitivity for this parameter, $\partial f/\partial w_1$ is −0.279 GHz/mm. The graph is also shifted left when the width is increased.
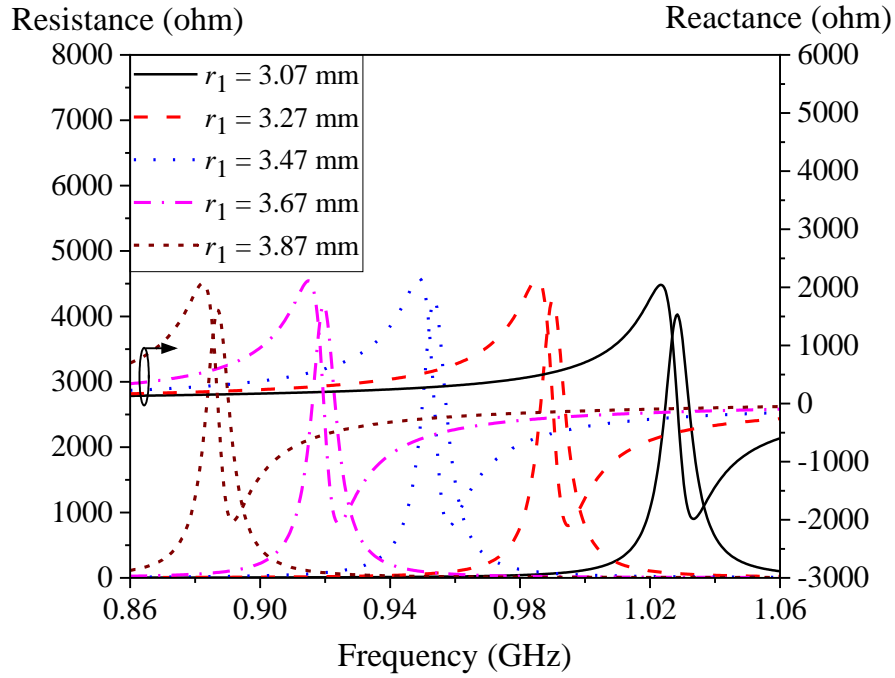
Figure 4.8: Effects of changing the radius, r_1 of the arc segment in Layer 1 and Layer 3. Other parameters remain unchanged.
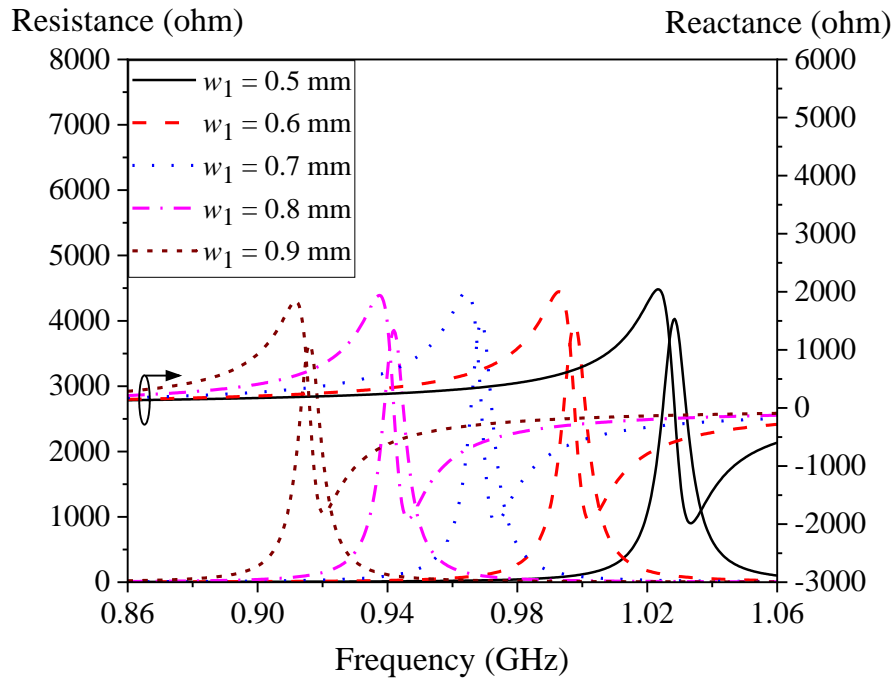
Figure 4.9: Effects of changing the width, w_1 of the arc segment in Layer 1 and Layer 3. Other parameters remain unchanged.

4.3.2   Patch Dimensions

Besides, the effects of changing the dimensions of the patches in Layer 1 and Layer 3 are also discussed and simulated impedance is plotted in Figure 4.10. With reference to Figure 4.10, longer patch width (w_p) makes the resistance decrease and the reactance to be more capacitive when other parameters remain unchanged. Changing w_p can adjust the inductive reactance at the rate of 1.19 kΩ/mm. It shows that changing the patch dimensions is helpful for adjusting the impedance matching of the tag antenna.
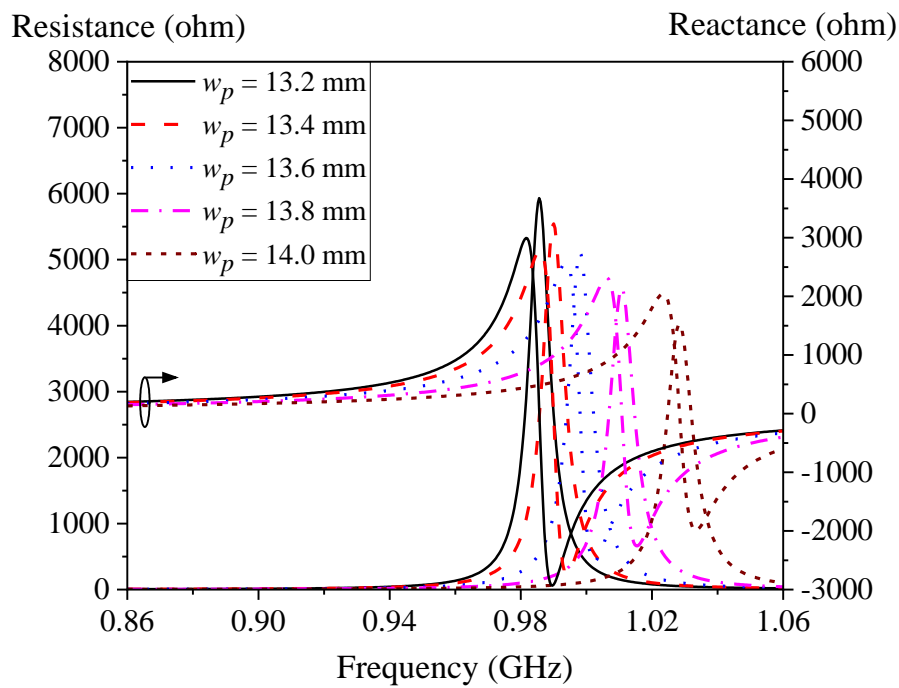
Figure 4.10: Effect of changing the dimensions (w_p) of the patches in Layer 1 and Layer 3. Other parameters remain unchanged.

4.3.3   Feeding Loop Radius

Furthermore, it is found that the antenna impedance is directly contributed by the feeding loop in Layer 2. The effects of changing the radius of the circular feeding loop (r_2) in Layer 2 are studied, the simulated impedance and power transmission coefficient are shown in Figures 4.11(a) and 4.11(b) respectively. With reference to Figure 4.11(a), the resonant frequency shifts rightward at a rate of 0.166 GHz for every 1 mm enlargement of r_2. The power transmission coefficient of the antenna remains stable at ~0.93 as shown in Figure 4.11(b). This shows that there is still achieve a good conjugate matching between the chip and tag antenna regardless of the alterations of this parameter.
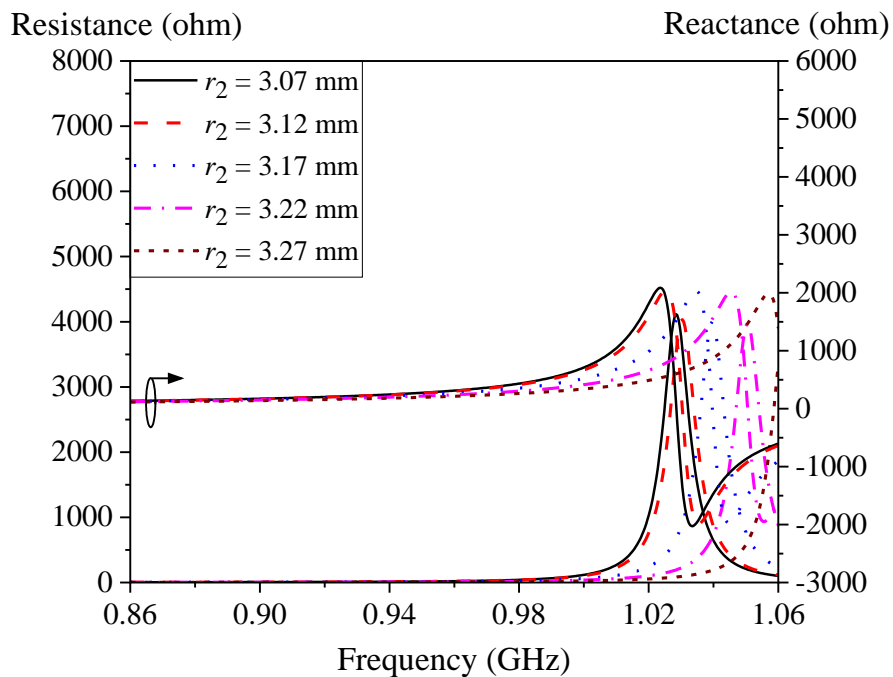
(a)

Figure 4.11: Effects of varying the radius (r_2) of the feeding loop on (a) input impedance and (b) power transmission coefficient.

4.3.4 Feeding Loop Width

At last, the effects of changing the width of the circular feeding loop (w_2) in Layer 2 are also discussed and the input impedance are shown in Figures 4.12(a) and 4.12(b). The antenna reactance is reducing at a rate of 0.24 kΩ for every 1 mm increment of w_2 as illustrated in Figure 4.12(a). Referring to Figure 4.12(b), it is observed that increasing the w_2 causes the reduction of resonant frequency and increment of the power transmission coefficient at the same time, making this parameter useful for fine-tuning purpose.
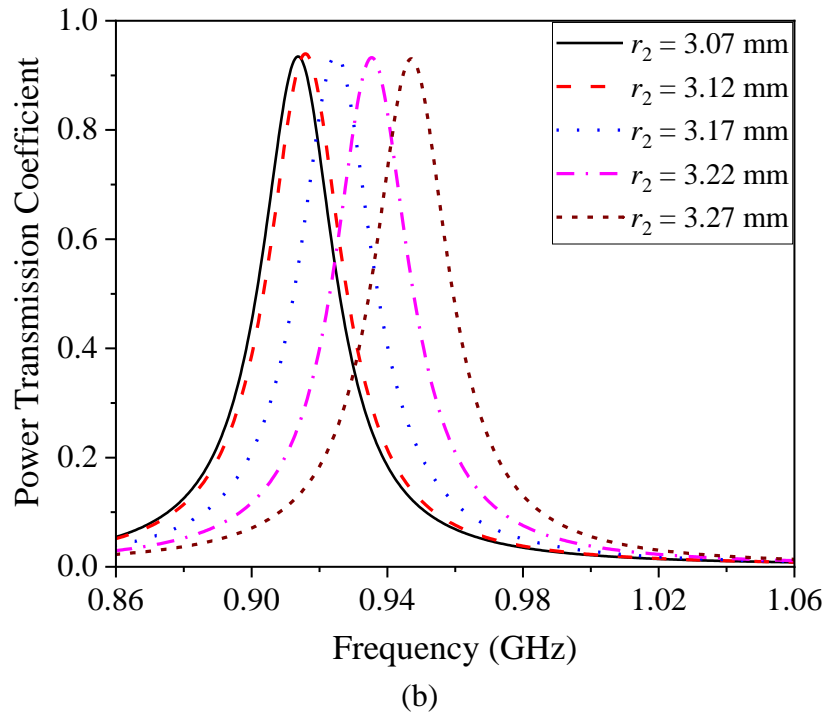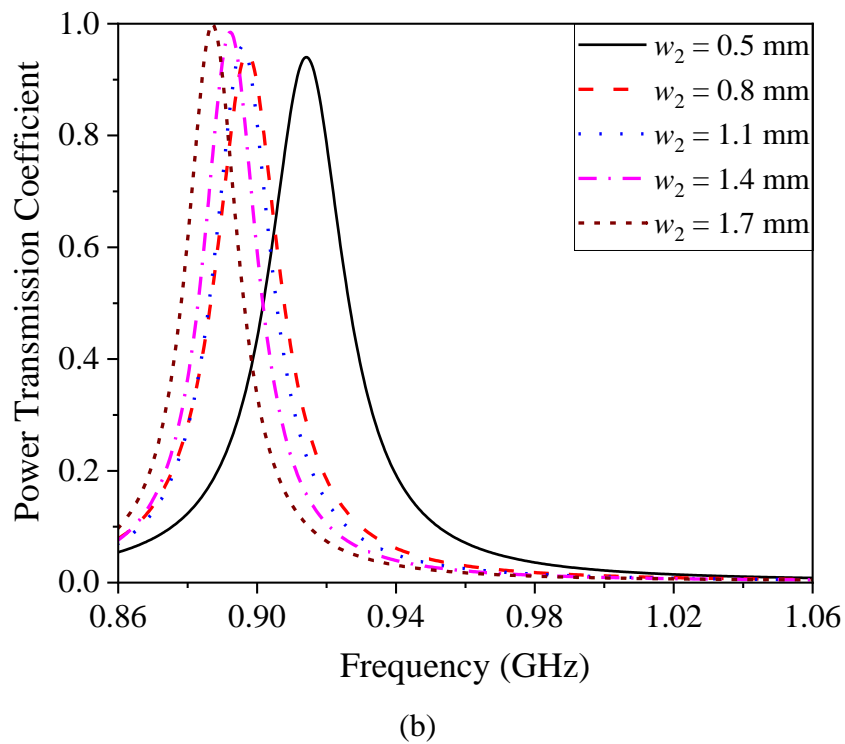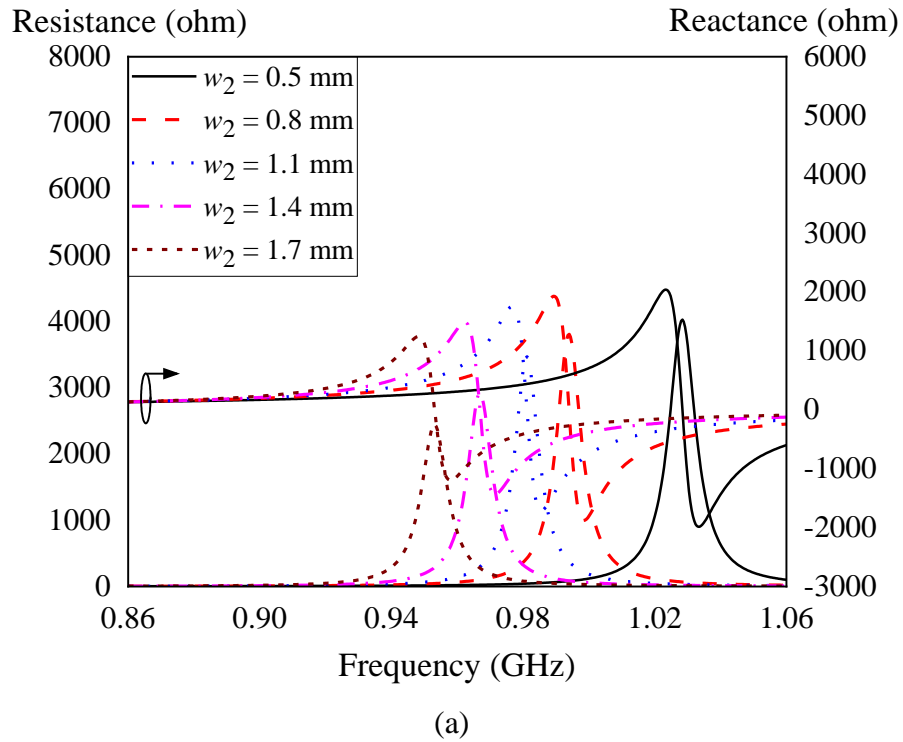
(a)

(b)

Figure 4.12: Effects of changing the width (w_2) of the feeding loop on (a) input impedance and (b) power transmission coefficient.

CHAPTER 5

CONCLUSION AND RECOMMENDATIONS

5.1   Conclusion

In this study, a new type of compact metal-mountable UHF RFID tag antenna has been proposed. The proposed tag antenna has a compact size and low profile. Four shorted patches of the proposed tag antenna are divided into two individual layers (Layer 1 and Layer 3) and placed in a rotational symmetry manner. The arc segment that connects the patches within the same layer can easily introduce additional inductance and lower down the resonance frequency of the proposed tag antenna. When mounted on a metal, it is able to produce a stable omnidirectional radiation pattern with a realized gain of -9.02 dBi and achievable read distance up to 6.25 m in all directions. This is very useful for applications that require full spatial sensing capability. The proposed antenna has a simulated resonant frequency of 914 MHz which can be used within the UHF band. The antenna has a high power transmission coefficient (>93%) as it is conjugately matched with the chip impedance. As a result, all the pre-requirements of this study are matched with the proposed tag antenna.

5.2   Recommendations for Future Work

A recommendation can be made to enhance this project in the future. The current operation bandwidth of the proposed antenna is from 911 MHz to 917 MHz, which can be further improved so that the tag antenna has a broader bandwidth selection.

CHAPTER 6

REFERENCES

Saba, Rita; Deleruyelle, Thibaut; Alarcon, Juvenal; Egels, Matthieu; Pannier, Philippe (2012 - 2012): *A resistant textile tag antenna for RFID UHF frequency band*. In : 2012 IEEE International Conference on RFID-Technologies and Applications (RFID-TA). 2012 IEEE International Conference on RFID-Technologies and Applications (RFID-TA). Nice, France, 5/11/2012 - 7/11/2012: IEEE, pp. 203–207.

Zhang, Y. J., Li, P., Zeng, H. N. and Song Tong, M., 2019 - 2019. *Design of a Tunable UHF RFID Tag Based on Rectangular Loop Antennas for Metallic Objects*. In: 2019 Photonics & Electromagnetics Research Symposium - Fall (PIERS - Fall). 2019 Photonics & Electromagnetics Research Symposium - Fall (PIERS - Fall). Xiamen, China, 17/12/2019 - 20/12/2019: IEEE, pp. 300–306.

Lee, Y.-H., Lim, E.-H., Bong, F.-L. and Chung, B.-K., 2019. *Compact Folded C-Shaped Antenna for Metal-Mountable UHF RFID Applications*. *IEEE Transactions on Antennas and Propagation,* [e-journal] 67(2), pp. 765–773. http://dx.doi.org/10.1109/TAP.2018.2879853.

Althobaiti, T., Sharif, A., Ouyang, J., Ramzan, N. and Abbasi, Q. H., 2020. *Planar Pyramid Shaped UHF RFID Tag Antenna With Polarisation Diversity for IoT Applications Using Characteristics Mode Analysis*. *IEEE Access,* e-journal] 8, pp. 103684–103696. http://dx.doi.org/10.1109/ACCESS.2020.2999256.

Lee, Y.-H., Moh, C.-W., Lim, E.-H., Bong, F.-L. and Chung, B.-K., 2020. *Miniature Folded Patch With Differential Coplanar Feedline for Metal Mountable UHF RFID Tag*. *IEEE Journal of Radio Frequency Identification,* [e-journal] 4(2), pp. 93–100. http://dx.doi.org/10.1109/JRFID.2019.2957011.

Lee, Y.-H., Lim, E.-H., Bong, F.-L. and Chung, B.-K., 2020. *Loop-fed Planar Inverted-L Antennas (PILAs) for Omnidirectional UHF On-Metal Tag Design*. *IEEE Transactions on Antennas and Propagation,* p. 1–1. http://dx.doi.org/10.1109/TAP.2020.2990287.

He, Y., Li, Y., Zhu, L. and Chen, P.-Y., 2020. *Miniaturization of Omnidirectional Cavity Antennas Using Substrate-Integrated Impedance Surfaces*. *IEEE Transactions on Antennas and Propagation,* p. 1–1. http://dx.doi.org/10.1109/TAP.2020.3012493.

Wong, K.-L., Su, S.-W. and Tang, C.-L., 2005. *Broadband omnidirectional metal-plate monopole antenna. IEEE Transactions on Antennas and Propagation,* [e-journal] 53(1), pp. 581–583. http://dx.doi.org/10.1109/TAP.2004.838765.

Cisco. 2020. *Omni Antenna vs. Directional Antenna - Cisco.* [ONLINE] Available at: https://www.cisco.com/c/en/us/support/docs/wireless-mobility/wireless-lan-wlan/82068-omni-vs-direct.html#topic3. [Accessed 02 September 2020].

Lee, S.-R., Ng, W.-H., Lim, E.-H., Bong, F.-L. and Chung, B.-K., 2020. *Compact Magnetic Loop Antenna for Omnidirectional On-Metal UHF Tag Design. IEEE Transactions on Antennas and Propagation,* [e-journal] 68(2), pp. 765–772. http://dx.doi.org/10.1109/TAP.2019.2943426.

Lin, Y.-F., Chen, H.-M., Lin, C.-Y. and Pan, S.-C., 2009. *Planar Inverted-L Antenna With a Dielectric Resonator Feed in a Mobile Device. IEEE Transactions on Antennas and Propagation,* [e-journal] 57(10), pp. 3342–3346. http://dx.doi.org/10.1109/TAP.2009.2029379.

Alja'afreh, S. S., Huang, Y. and Xing, L., 2014 - 2014. *A compact, wideband and low profile planar inverted-L antenna.* In: *The 8th European Conference on Antennas and Propagation (EuCAP 2014). 2014 8th European Conference on Antennas and Propagation (EuCAP).* The Hague, Netherlands, 6/4/2014 - 11/4/2014: IEEE, pp. 3283–3286.

Shin-Rou Lee, Eng-Hock Lim, Fwee-Leong Bong, Boon-Kuan Chung and Kim-Yee Lee, 2018. *Proceedings of the 2018 IEEE 7th Asia-Pacific Conference on Antennas and Propagation (APCAP): 5-8 August 2018, New Zealand. [e-book].* Piscataway, NJ: IEEE. <http://ieeexplore.ieee.org/servlet/opac?punumber=8509819>.

Ng, W.-H., Lim, E.-H., Bong, F.-L. and Chung, B.-K., 2019. *Compact Planar Inverted-S Antenna With Embedded Tuning Arm for On-Metal UHF RFID Tag Design. IEEE Transactions on Antennas and Propagation,* [e-journal] 67(6), pp. 4247–4252. http://dx.doi.org/10.1109/TAP.2019.2911191.

ECCOSTOCK PP. Accessed: Sep. 2020. [Online]. Available: http://www.eccosorb.com/Collateral/Documents/English-US/PP.pdf

Monza 5 Tag Chip Datasheet, Rev 3.0. Accessed: Aug. 9, 2020. [Online]. Available: https://support.impinj.com/hc/en-us/articles/202756948- Monza-5-Tag-Chip-Datasheet

Lee, Yong-Hong; Lim, Eng-Hock; Bong, Fwee-Leong; Chung, Boon-Kuan; Lee, Kim-Yee (2019 - 2019): *Complementary Planar Inverted-F Antennas (PIFAs) for On-Metal RFID Tag Design*. In : 2019 IEEE Asia-Pacific Conference on Applied Electromagnetics (APACE). 2019 IEEE Asia-Pacific Conference on Applied Electromagnetics (APACE). Melacca, Malaysia, 25/11/2019 - 27/11/2019: IEEE, pp. 1–3.

Erman, Fuad; Hanafi, Effariza; Lim, Eng-Hock; Mahyiddin, Wan Amirul Wan Mohd; Harun, Sulaiman Wadi; Umair, Hassan; Soboh, Rawan (2020): *U-Shaped Inductively Coupled Feed UHF RFID Tag Antenna With DMS for Metal Objects*. In *Antennas Wirel. Propag. Lett.* 19 (6), pp. 907–911. DOI: 10.1109/LAWP.2020.2981960.

Dakhli, Nabil; Choubani, Fethi (2019 - 2019): *Dual Band Metamaterial Inverted-L Antenna*. In : 2019 IEEE 19th Mediterranean Microwave Symposium (MMS). 2019 IEEE 19th Mediterranean Microwave Symposium (MMS). Hammamet, Tunisia, 31/10/2019 - 2/11/2019: IEEE, pp. 1–4.

Ng, Wai-Hau; Lim, Eng-Hock; Bong, Fwee-Leong; Chung, Boon-Kuan (2019): *E-Shaped Folded-Patch Antenna With Multiple Tuning Parameters for On-Metal UHF RFID Tag*. In *IEEE Trans. Antennas Propagat.* 67 (1), pp. 56–64. DOI: 10.1109/TAP.2018.2874795.

Rogerscorp.com. 2020. RT/Duroid® 6006 And 6010.2LM Laminates - Rogers Corporation. [online] Available at: <https://rogerscorp.com/advanced-connectivity-solutions/rt-duroid-laminates/rt-duroid-6006-and-6010-2lm-laminates> [Accessed 10 September 2020].

Carl. P, "Fundamental efficiency limits for small metallic antennas," *IEEE Trans. Antennas Propag.*, vol. 65, no. 4, pp. 1642-1650, Apr. 2017.

Andrew. J. Compston, J. D. Fluhler and H. G. Schantz, "A Fundamental Limit on Antenna Gain for Electrically Small Antennas," *2008 IEEE Sarnoff Symposium*, Princeton, NJ, USA, 2008, pp. 1-5, doi: 10.1109/SARNOF.2008.4520113.

Hertleer, Carla. (2009). "Design of planar antennas based on textile materials."

Puri, S., Kaur, K. and Kumar, N. (2014) 'A Review of Antennas for Wireless Communication Devices', *International Journal of Electronics and Electrical Engineering*, pp. 199–201.

Electronics notes. 2021. Antenna Resonance: Radio Aerial Bandwidth » Electronics Notes. [ONLINE] Available at: https://www.electronics-notes.com/articles/antennas-propagation/antenna-theory/resonance-bandwidth.php#:~:text=A%20radio%20antenna%20is%20a,reactances%20cancel%20each%20other%20out.. [Accessed 26 March 2021].

ECS, Inc. International. 2021. What is Resonant Frequency? - ECS Inc. International. [ONLINE] Available at: https://ecsxtal.com/news-resources/video-learning/126-everything-you-need-to-know-about-quartz-crystal-resonators/129-understanding-resonant-frequency. [Accessed 26 March 2021].